Materials Science in Semiconductor Processing 74 (2018) 369–374

Contents lists available at ScienceDirect

Materials Science in Semiconductor Processing

journal homepage: www.elsevier.com/locate/mssp

Growth and ripening of oxygen precipitation in neutron-irradiated Czochralski silicon

Peng Wang[a,b], Can Cui[a,b,*], Xuegong Yu[b], Deren Yang[b]

[a] Center for Optoelectronics Materials and Devices, Department of Physics, Zhejiang Sci-Tech University, Hangzhou 310018, China
[b] State Key Laboratory of Silicon Materials, School of Materials Science and Engineering, Zhejiang University, Hangzhou 310027, China

ARTICLE INFO

Keywords:
Silicon
Neutron-irradiation
Vacancy-related defects
Oxygen precipitation

ABSTRACT

The effects of the vacancy-related defects introduced by neutron irradiation on oxygen precipitation in Czochralski silicon have been elaborately investigated. It is found that the vacancy-related defects significantly enhance the nucleation of oxygen precipitates as well as the growth of the grown-in oxygen precipitates. The Ostwald ripening of oxygen precipitates in neutron-irradiated silicon wafers is observed during a low-high two-step annealing. It is interpreted that the vacancy-related defects facilitate the formation of platelet-like oxygen precipitates, which continue to grow at the expense of small-sized oxygen precipitates during the high temperature annealing process. However, when subjected to the subsequent rapid thermal annealing at higher temperature, the platelet-like oxygen precipitates in the neutron-irradiated silicon exhibit lower stability due to the large surface free energy.

1. Introduction

Oxygen is inevitably incorporated into Czochralski (CZ) silicon from the quartz crucible during the crystal growth. The supersaturated oxygen atoms can form oxygen precipitates during the cooling or annealing process, and even further induce secondary defects such as dislocations, stacking faults, which are all termed as bulk micro-defects (BMDs). The BMDs can serve as sinks to getter metal impurities in the fabrication of integrated circuits, with a denuded zone (DZ) formed by oxygen out-diffusion from silicon wafer surface at high temperature [1–3]. As semiconductor devices are becoming more and more integrated and compact for higher and more stable performance, the elimination of metal impurities from the active regions of the device is of great importance in ultra large scaled integrated technology [4–6]. It is well known that the BMD density in CZ silicon is proportional to the density of oxygen precipitates [7,8]. To optimize the internal gettering, many studies have been reported on the nucleation and growth of oxygen precipitates. The oxygen precipitation in CZ silicon crystal can be affected by initial interstitial oxygen concentration ($[O_i]$) [9], crystal growth history [10,11], doped impurities [12–14], point defects [15–17], and thermal treatment procedures [18].

As a type of important intrinsic point defects in silicon crystal, vacancies can improve both the nucleation and growth of oxygen precipitates [15,19]. The formation of V_nO_m ($n, m \geq 1$) complexes are considered to be the heterogeneous nucleation centers of oxygen precipitates. However, the grown-in vacancy concentration ([V]) is insufficient for oxygen precipitation to occur spontaneously in CZ silicon for modern integrated circuits. Hence, a rapid thermal annealing (RTA) at high temperature (normally above 1100 °C) has been developed to intentionally introduce relatively high concentration vacancies [20,21]. The vacancies significantly enhance oxygen precipitates during the subsequent heat treatments [22], improving the internal gettering capacity of CZ silicon wafers [23,24]. However, the [V] introduced during crystal growth or RTA at high temperature is seriously limited by its solubility [25,26].

Neutron or electron irradiation has been reported to introduce high concentration vacancies in silicon crystal at room temperature (RT) [27–29], where the [V] is dependent on the dose and bombarding energy of the neutron or electron. Generally, vacancies and self-interstitials are formed simultaneously during particle irradiation, while most of them are annihilated through recombination reaction and a part of them form different defect complexes with impurities [30,31]. The A-center (VO complex) is known to be the predominant defect complex in the neutron irradiated silicon [32]. Upon thermal annealing (< 650 °C), VO is converted into various V_nO_m complexes with the addition of vacancies and/or oxygen atoms, which can be manipulated by isovalent doping [30,33–35]. Large V_nO_m complexes could act as nuclei centers to enhance oxygen precipitation in irradiated silicon for an effective internal gettering process [36]. Our previous work has demonstrated that V_nO_m complexes improve oxygen precipitation

* Corresponding author at: Center for Optoelectronics Materials and Devices, Department of Physics, Zhejiang Sci-Tech University, Hangzhou 310018, China.
E-mail address: cancui@zstu.edu.cn (C. Cui).

https://doi.org/10.1016/j.mssp.2017.11.010
Received 20 July 2017; Received in revised form 17 October 2017; Accepted 8 November 2017
Available online 16 November 2017

during the annealing process in a wide temperature range, and interestingly a well-defined internal gettering structure with the DZ and dense BMDs is formed in neutron-irradiated CZ silicon by a single-step high temperature annealing [37,38]. Furthermore, it was reported that the internal gettering efficiency can be significantly affected by the morphology of oxygen precipitates [39,40]. The most frequently reported morphologies of oxygen precipitates in silicon are plate-like, octahedral and spherical. Kot et al. have observed three dimensional dendrites formed in vacancy-rich CZ silicon pre-treated by RTA [41]. However, there is lack of knowledge about the influence of vacancies on the morphologies of oxygen precipitates and their evolution behaviors in the thermal annealing processes, especially in irradiated silicon.

In this work, we investigate oxygen precipitation behaviors in neutron irradiated CZ silicon crystal subjected to a low-high two-step annealing and a subsequent RTA, respectively. The nucleation of oxygen precipitates is significantly enhanced by the vacancy-related defects, and the Ostwald ripening of oxygen precipitates in the irradiated silicon is observed during the high temperature annealing. It is considered that the vacancy-related defects facilitate the formation of platelet-like oxygen precipitates, which continue to grow up at the expense of small-sized oxygen precipitates during the prolonged high temperature annealing. These platelet-like oxygen precipitates are less stable in subsequent RTA at higher temperature and could be easily dissolved.

2. Experimental

A *n*-type phosphorus-doped < 111 > silicon crystal grown by the CZ method was used in our experiment. A portion of the silicon crystal was subjected to 1 MeV fast neutron irradiation at RT with a flux of 1.83×10^{13} cm^{-2}. The initial [O_i] and [V] in the samples are summarized in Table 1, where the neutron-irradiated CZ silicon is named as NICZ silicon. The initial [O_i] was determined by a Fourier transform infrared (FTIR) spectrometer with a calibration coefficient of 3.14×10^{17} cm^{-2} (ASTM F 121-89 standard). Based on the 830 cm^{-1} absorption line related to A-center in FTIR spectra, the [V] (including all the vacancy-related complexes) in the NICZ silicon was calculated to be above 1×10^{16} cm^{-3} using a calibration coefficient of 6.1×10^{16} cm^{-2} [42]. This concentration is much higher than the thermal equilibrium [V] in silicon at melting point, which equals to 10^{15} cm^{-3} [25].

The CZ and NICZ silicon wafers were first subjected to a low-high two-step annealing of 650 °C, 8 h + 1050 °C, 16 h in argon atmosphere. It should be noted that the ramped rate from 650 °C to 1050 °C was 1 °C/min, which is slow enough to enable the growth of new oxygen precipitates as well as grown-in oxygen precipitates. During the annealing process at 1050 °C, some samples were taken out of the furnace at different time intervals for the FTIR measurement. After the FTIR measurement, the samples were etched in HNO_3/HF (HNO_3:HF = 3:1) solution to remove a layer about 100-micron thick from both surfaces and then etched in Sirtl etchant (10 g CrO_3: 20 mL HF: 20 mL H_2O) for 4 min (the etch removal is ~ 5 μm). The BMDs were observed with an optical microscope (Olympus MX-50). Furthermore, some of the 650 °C, 8 h + 1050 °C, 16 h thermal treated samples were subsequently subjected to a RTA at 1250 °C for 50 s in argon atmosphere to investigate the thermal stability of oxygen precipitates.

Oxygen precipitates with different morphologies result in different

Table 1
Initial interstitial oxygen concentration ([O_i]), neutron irradiation dose and vacancy concentration ([V], including all the vacancy-related defects) for the samples.

Sample	[O_i] (cm^{-3})	Neutron irradiation[a] dose (cm^{-2})	[V] (cm^{-3})
CZ	9.3×10^{17}	–	–
NICZ	9.5×10^{17}	1.83×10^{13}	$> 1 \times 10^{16}$

[a] fast neutron irradiation was done at room temperature with energy of 1 MeV.

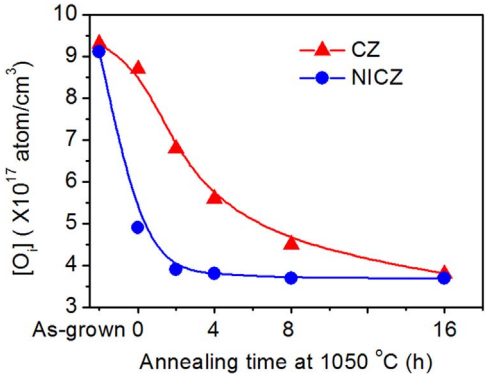

Fig. 1. Dependence of [O_i]s in the CZ and NICZ silicon on the annealing time at 1050 °C following the pre-annealing at 650 °C for 8 h.

absorption lines in IR spectra, which can be easily distinguished when measured at liquid helium temperature, as a result of the shrinkage of the full width at half maximum (FWHM) of the O_i related absorption line [43–46]. To characterize the oxygen precipitates in CZ and NICZ silicon crystal, the thermal treated samples were examined by low temperature FTIR measurements in a Bruker IFS 66 v/S instrument equipped with a Globar source, a KBr beam splitter and a deuterated triglycine sulfate detector with high sensitivity. The measurements were performed at 10 K using a liquid helium Oxford Optistat with two KRS5 windows. The resolution was set to be 0.5 cm^{-1} and 128 scans were accumulated for each spectrum to improve the signal to noise ratio.

3. Results and discussion

3.1. Enhanced oxygen precipitation nucleation in neutron-irradiated silicon

The CZ and NICZ silicon samples were subjected to a two-step annealing to form oxygen precipitates, including annealing at 650 °C for 8 h and annealing at 1050 °C with various time intervals. Fig. 1 shows the variation of [O_i] depending on the annealing time at 1050 °C following the 650 °C pre-annealing for 8 h. In the CZ silicon, the [O_i] decreases gradually and reaches an equilibrium concentration at 16 h. However, in the NICZ silicon, the [O_i] decreases more rapidly and achieves the equilibrium concentration at 2 h. As expected, the oxygen precipitation in the NICZ silicon is greatly enhanced at the early annealing stage by the neutron irradiation introduced vacancy-related defects.

In general, the A-centers are the dominant vacancy-related defects in CZ silicon after 1 MeV neutron irradiation, which are not stable during subsequent annealing process [42]. Some of them transform into more complicated complexes V_nO_m and the others decompose into V and O_i. In the NICZ silicon crystal, the [VO] is about 1×10^{16} cm^{-3}, evaluated from FTIR measurement. High density V_nO_m complexes are expected to generate during the 650 °C annealing [34], which would act as nuclei centers for oxygen precipitation in the ramped annealing process and the subsequent annealing at 1050 °C. Therefore, a sharp reduction of [O_i] in NICZ silicon is observed as the temperature ramped to 1050 °C from 650 °C (Fig. 1). On the other hand, the decomposed vacancies could also facilitate the growth of oxygen precipitate nuclei by providing space to relieve the strain arising from the oxygen precipitate growth.

Moreover, the growth of the grown-in oxygen precipitates plays another important role during the low-high two-step annealing. Based on the previous report [47], the critical radius for oxygen precipitate growth in the subsequent annealing process depends particularly on the [V]. With the [V] in the NICZ silicon crystal increasing, the critical radius for oxygen precipitate growth at a certain temperature reduces, resulting in more grown-in oxygen precipitates, which would survive

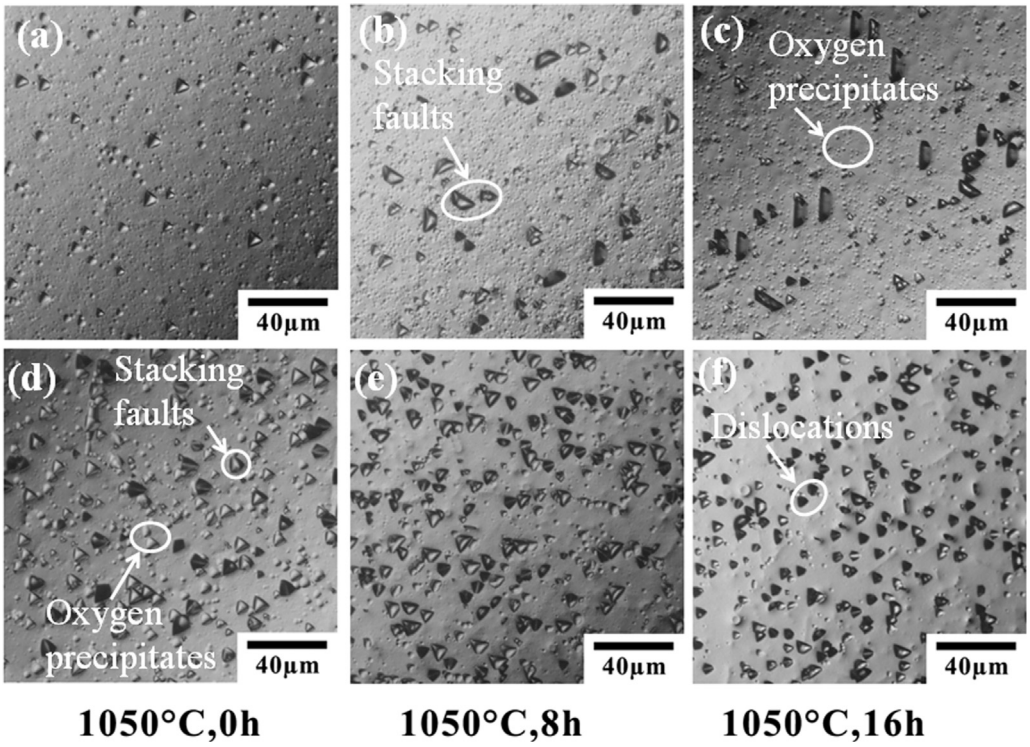

Fig. 2. Representative optical micrographs of the BMDs in the CZ (a-c) and NICZ (d–f) silicon subjected to two-step annealing by 8 h pre-annealing at 650 °C and various annealing time at 1050 °C, respectively.

and grow up during the subsequent high temperature annealing.

3.2. Ostwald ripening of oxygen precipitates in neutron-irradiated silicon

During the 1050 °C annealing, the BMD densities in the CZ and NICZ silicon were investigated by preferential chemical etching, as shown in Fig. 2. The corresponding densities of different defects (oxygen precipitates, dislocations and stacking faults) are calculated based on the numbers of etch pits and summarized in Table 2. At the early stage of the annealing, the oxygen precipitate density in the NICZ silicon (Fig. 2d) is lower than that in the CZ silicon (Fig. 2a), while the reduction of [O_i] in the former is more than that in the latter (Fig. 1). It indicates that high density and small-sized oxygen precipitates are generated in the CZ silicon, but relatively low density and large-sized oxygen precipitates are created in the NICZ silicon during the two-step annealing. In other words, the oxygen precipitation is greatly enhanced by heterogeneous nuclei centers of vacancy-related defects (V_nO_m complexes) in NICZ silicon.

As the annealing time prolongs, the change of the oxygen precipitate density in such two kinds of silicon is obviously different, i.e., the oxygen precipitate density reduces slightly in the CZ silicon whereas it decreases dramatically in the NICZ silicon. The experiment has been repeated for several times to confirm that the crucial difference in change tendency of the oxygen precipitate density is not a random phenomenon. It is found that the [O_i] remains nearly constant during the 1050 °C annealing over 2 h (Fig. 1), whereas the oxygen precipitate density decreases 2–3 times in the NICZ silicon (Table 2). In comparison with a similar phenomenon occurred in the nitrogen-doped silicon crystal [48], it is interpreted that the prolonged annealing at high temperature leads to a continued growth of larger oxygen precipitates and a progressive loss of the smaller precipitates due to their dissolution. This process minimizes the total interface energy of the system, which is a well-known process in metallurgy called as Ostwald ripening [49]. It is worth to note that the slight reduction of oxygen precipitate density in CZ silicon is also ascribed to the Ostwald ripening process.

Extended defects are found to generate around the oxygen precipitates, such as dislocations and stacking faults (Fig. 2). The densities of extended defects increase with the increasing annealing time at 1050 °C, and they are higher in the NICZ silicon than in the CZ silicon (Table 2). The reason is that the oxygen precipitates can introduce large strain and deform the silicon lattice, resulting in numerous silicon interstitials which are pushed out and aggregate to form such extended defects. The larger-sized oxygen precipitates lead to more extended defects formed in the NICZ silicon. It should be noted that the ultra-large stacking faults are observed in the CZ silicon after 1050 °C, 16 h annealing, as shown in Fig. 2c, which indicates inhomogeneous silicon interstitial ejection from oxygen precipitates in the sample.

Fig. 3 shows the FTIR spectra of the CZ (a) and NICZ silicon (b) subjected to annealing at 1050 °C with various annealing time following pre-annealing at 650 °C for 8 h, measured at RT. The IR absorption lines of oxygen precipitates are around 1227 cm^{-1}, and the absorbance intensity increases slightly as the annealing time increases in CZ silicon (Fig. 3a). Whereas, it is clearly observed in NICZ silicon that the IR absorption line of oxygen precipitates shifts from 1230 to 1214 cm^{-1} and its intensity increases gradually, with the annealing time increasing (Fig. 3b). It should be noted that the intensity of the O_i

Table 2
The densities of BMDs (oxygen precipitates, dislocations, stacking faults) in the CZ (a-c in Fig. 2) and NICZ (d-f in Fig. 2) silicon subjected to the two-step annealing with 8 h pre-annealing at 650 °C and various annealing time at 1050 °C.

	a	b	c	d	e	f
oxygen precipitates (10^{10} cm^{-3})	1.5 ± 0.1	1.4 ± 0.1	1.2 ± 0.1	0.7 ± 0.1	0.5 ± 0.1	0.23 ± 0.01
dislocations (10^8 cm^{-3})	2.3 ± 1.9	3.1 ± 1.2	4.8 ± 1.5	5.2 ± 3.0	7.1 ± 2.0	8.7 ± 0.9
stacking faults (10^8 cm^{-3})	2.3 ± 0.9	4.1 ± 0.9	4.3 ± 0.6	7.3 ± 0.5	8.5 ± 0.4	8.7 ± 1.1

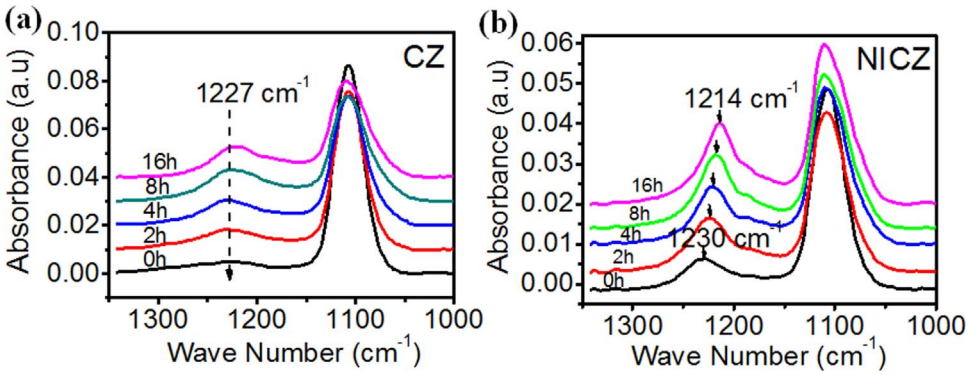

Fig. 3. FTIR spectra of the CZ (a) and NICZ silicon (b) subjected to two-step annealing with various annealing time at 1050 °C following 8 h pre-annealing at 650 °C, measured at RT.

related absorption line around 1107 cm^{-1} remains nearly constant as the annealing time exceeds 2 h. It was proposed that the IR absorption line around 1230 cm^{-1} is related to platelet-shaped oxygen precipitates [43]. It was also suggested by Gryse et al. [45] that the IR absorption line shift in the frequency is not due to a differing stoichiometry, but to a different geometrical structure of the composite, of which the reduced spectral function is the emanation. So the FTIR spectra indicates oxygen precipitates experience shape transformation from thin-platelet to thick-platelet (maybe more accurately from asymmetric shapes to more symmetric shapes) along with the high temperature annealing. The increase of the precipitate sizes during the high temperature annealing may also contribute to the shift of the IR absorption line. The increased intensity and the shrinkage of FWHM of the IR line related to oxygen precipitates during the high temperature annealing strongly suggest the formation of oxygen precipitates with more homogeneous shape in the NICZ silicon.

Fig. 4a compares the FTIR spectra of the CZ and NICZ samples after 650 °C, 8 h + 1050 °C, 16 h two-step annealing, measured at RT. It can be seen that the IR absorption line around 1214 cm^{-1} in the NICZ silicon is narrower and higher than that in the CZ silicon, indicating more homogeneous platelet-shaped oxygen precipitates formed in the NICZ silicon. Nevertheless, the IR absorption line (around 1085 cm^{-1}) related to the sphere-shaped oxygen precipitates is overlapped with the strong absorption line of O_i around 1107 cm^{-1} and cannot be distinguished clearly. The FTIR measurement at liquid helium temperature is an effective way to characterize the morphology distribution of oxygen precipitates (including platelet- and sphere-shaped oxygen precipitates) in silicon crystal [42–44,50]. Fig. 4b shows the FTIR spectra of the corresponding CZ and NICZ samples at 10 K. Except for the main IR absorption line of O_i at 1136 cm^{-1}, the other two IR absorption lines around 1100 and 1214 cm^{-1} corresponding to sphere- and platelet-shaped oxygen precipitates are observed, respectively. A subtraction of the two FTIR spectra is also shown in the Fig. 4b, which display a convex peak at 1100 cm^{-1} and a concave peak at 1214 cm^{-1}. It confirms that there are more platelet-like oxygen precipitates but less spherical oxygen precipitates in the NICZ silicon compared to the CZ silicon sample.

Based on the above discussions, it is concluded that the incorporation of vacancy-related defects in the NICZ silicon promotes the formation of platelet-like oxygen precipitates, which continue to grow up at the expense of small-sized oxygen precipitates during the high temperature annealing. Whereas, in the CZ silicon, there exist both sphere- and platelet-shaped oxygen precipitates, with relatively small sizes but higher densities than that in NICZ silicon (see Fig. 2c and f). In the previous report [46], it is well recognized that the morphology of oxygen precipitate correlates with the annealing temperature and annealing procedure. Our experiments provide a straight evidence that the vacancies can also strongly affect the morphology of oxygen precipitates. Furthermore, our experimental results are in great agreement with the theoretical expectation proposed by Voronkov et al. [51] that high concentration vacancies favored the growth of platelet-like precipitates rather than spherical precipitates, considering the competition of strain energy and surface free energy during the precipitate growth.

3.3. Thermal stability of oxygen precipitates in neutron-irradiated silicon

RTA at high temperature not only introduces high vacancy concentration in silicon wafer, but also impacts oxygen precipitate dissolution [52,53]. After the low-high two-step annealing, the samples were subjected to a RTA treatment to evaluate the thermal stability of the oxygen precipitates. Fig. 5a shows the variation of the $[O_i]$ for CZ and NICZ silicon samples during the multi-step annealing. The $[O_i]$ in the NICZ silicon almost recovers to its initial value, while in the CZ silicon it only recovers 60% after the multi-step annealing. It indicates that more oxygen precipitates in the NICZ silicon are dissolved during the RTA treatment, in comparison with the CZ silicon. In another word,

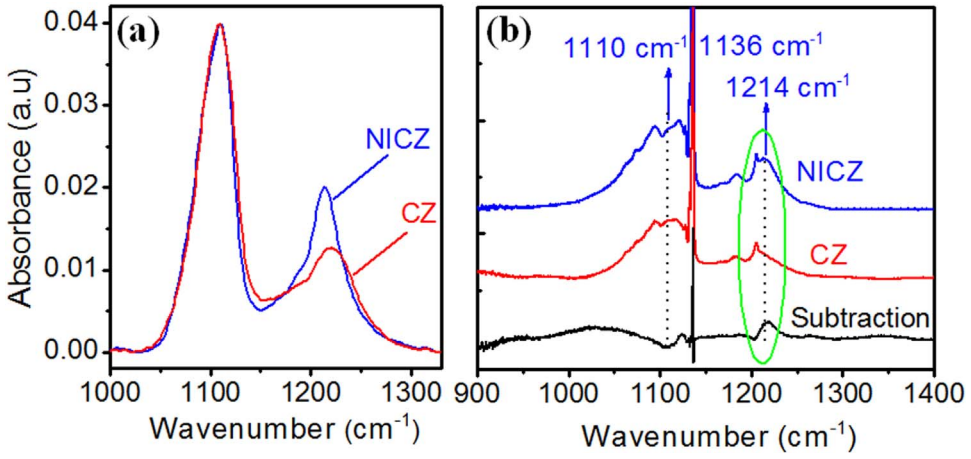

Fig. 4. FTIR spectra of the CZ and NICZ silicon after 650 °C, 8 h + 1050 °C, 16 h two-step annealing, measured at RT (a) and 10 K (b).

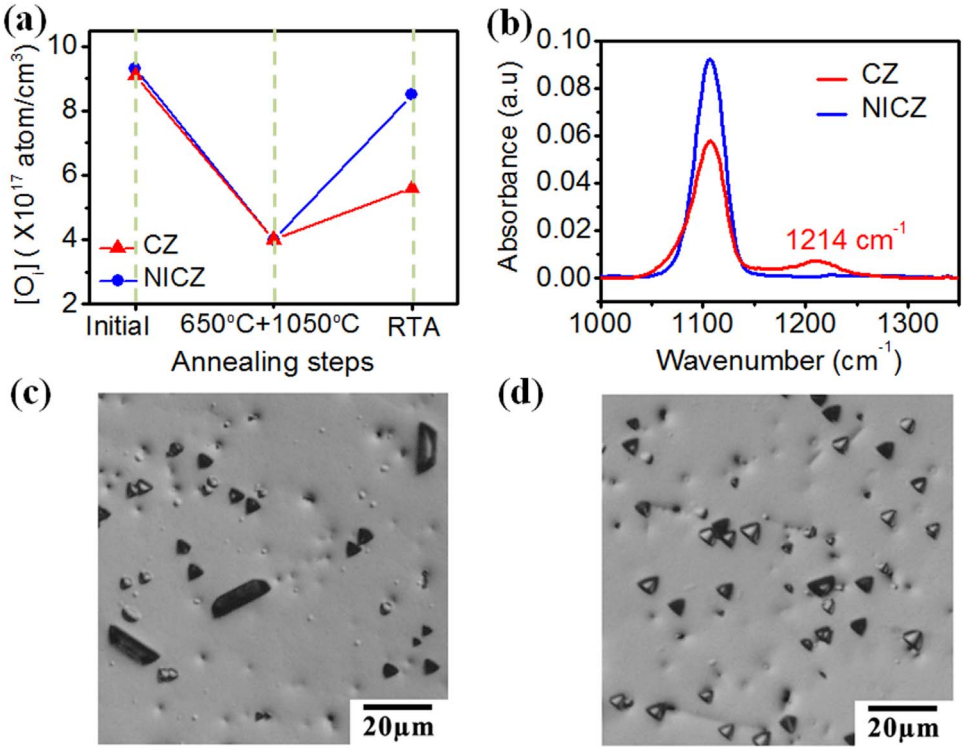

Fig. 5. (a) [O_i]s of the CZ and NICZ silicon during the multi-step annealing of 650 °C, 8 h + 1050 °C, 16 h + RTA (1250 °C, 50 s); (b) FTIR spectra of the CZ and NICZ silicon after multi-step annealing of 650 °C, 8 h + 1050 °C, 16 h + RTA (1250 °C, 50 s), and the representative optical micrographs of the CZ (c) and NICZ silicon (d).

it reveals that the oxygen precipitates in the NICZ silicon are less thermally stable than in the CZ silicon.

Fig. 5b, c and d show the FTIR spectra of the RTA treated CZ and NICZ silicon and their corresponding optical micrographs. After the RTA treatment, the oxygen precipitate related IR absorption line around 1214 cm^{-1} in both CZ and NICZ silicon decreases significantly (Fig. 5b), and the intensity of NICZ silicon is smaller than that of the CZ silicon. The oxygen precipitate densities of CZ (Fig. 5c) and NICZ samples (Fig. 5c) are 1.8 × 10^9 and 0.8 × 10^9 cm^{-3}, respectively, which are smaller than the ones before RTA treatment (Table 2). It confirms that the oxygen precipitates in these samples have been dissolved remarkably, and less oxygen precipitates are left in the NICZ silicon after the RTA treatment, in agreement with the variation of [O_i] in Fig. 5a and IR absorption line of oxygen precipitates in Fig. 5b. In addition, the dislocation density (4.5 × 10^8 cm^{-3}) and stacking fault density (4.3 × 10^8 cm^{-3}) of CZ sample remain almost the same as the values before RTA treatment, while the dislocation density (6.8 × 10^8 cm^{-3}) and stacking fault density (5.5 × 10^8 cm^{-3}) of NICZ sample reduce due to the relief of residual stress associated with the dissolving of more large-sized oxygen precipitates.

As previously discussed, the vacancy-related defects significantly enhance the formation of platelet-like oxygen precipitates in the NICZ silicon. These platelet-like oxygen precipitates possess larger surface free energy, which makes them dissolve more easily than the sphere-shape oxygen precipitates during the high temperature RTA treatment. Another possible reason might be ascribed to the high density extended defects (dislocations and stacking faults) in the NICZ silicon, which may assist the diffusion of decomposed O_i atoms towards the neighboring region with low [O_i] [54], and thus facilitate the dissolution of oxygen precipitates.

4. Conclusions

In summary, the effects of the vacancy-related defects introduced by neutron irradiation on oxygen precipitation in CZ silicon have been investigated. In a low-high two-step annealing, it is found that the vacancy-related defects significantly enhance the nucleation of oxygen precipitates as well as the growth of the grown-in oxygen precipitates. The Ostwald ripening of oxygen precipitates in the neutron-irradiated silicon wafers is observed during the high temperature annealing. It is interpreted that the vacancy-related defects improve the formation of platelet-like oxygen precipitates which continue to grow up at the expense of small-sized oxygen precipitates. Furthermore, these platelet-like oxygen precipitates as subjected to RTA at high temperature in the neutron-irradiated silicon are less stable due to the large surface free energy, and thus can be easily dissolved.

Acknowledgements

This project is supported by National Natural Science Foundation of China (No. 51532007, 61604131, 61574124), Science Challenge Project of National Defense Science, Technology and Industry Bureau of China (No. JCKY2016212A503) , Visiting Scholar Foundation of State Key lab of Silicon Materials (No. SKL2016-1), Science Foundation of Zhejiang Sci-Tech University (No. 16062067-Y), 521 Talents Project of Zhejiang Sci-Tech University.

References

[1] T.Y. Tan, E.E. Gardner, W.K. Tice, Appl. Phys. Lett. 30 (1977) 175.
[2] D. Gilles, E.R. Weber, S.K. Hahn, Phys. Rev. Lett. 64 (1990) 196.
[3] G. Kissinger, D. Kot, M.A. Schubert, A. Sattler, T. Müller, Solid State Phenom. 242 (2016) 236.
[4] S. Mahajan, MRS Bull. 40 (2015) 1079.
[5] G. Eranna, Crystal Growth and Evaluation of Silicon for VLSI and ULSI, CRC Press, New York, 2014.
[6] Y.-K. Choi, S.-Y. Jeong, B.-C. Sim, J. Korean Cryst. Growth Cryst. Technol. 26 (2016) 121.
[7] K. Moriya, K. Hirai, K. Kashima, S. Takasu, J. Appl. Phys. 66 (1989) 5267.
[8] G. Kissinger, J. Dabrowski, A. Sattler, C. Seuring, T. Müller, H. Richter, W. v. Ammonc, J. Electrochem. Soc. 154 (2007) H454.
[9] H.T.- Jaensch, D. Sieger, R. Geick, W. Zulehner, A. Geyer, Appl. Phys. A 54 (1992) 19.
[10] N.I. Puzanov, A.M. Eldenzon, Semicond. Sci. Technol. 7 (1992) 406.
[11] A.L. Donne, S. Binetti, V. Folegatti, G. Coletti, Appl. Phys. Lett. 109 (2016) 033907.
[12] X. Yu, D. Yang, X. Ma, J. Yang, L. Li, D. Que, J. Appl. Phys. 92 (2002) 188.
[13] J. Chen, D. Yang, H. Li, X. Ma, D. Que, J. Appl. Phys. 99 (2006) 073509.
[14] C. Gao, X. Ma, J. Zhao, D. Yang, J. Appl. Phys. 113 (2013) 093511.

[15] R. Falster, V.V. Voronkov, F. Quast, Phys. Stat. Sol. (B) 222 (2000) 219.
[16] A.J.R. Kock, W.M. Wijgert, Appl. Phys. Lett. 38 (1981) 888.
[17] A. Misiuk, B. Surma, C.A. Londos, J.B.- Misiuk, W. Wierzchowski, K. Wieteska, W. Graeff, Phys. Stat. Sol. (C) 2 (2005) 1812.
[18] S.M. Hu, J. Appl. Phys. 52 (1981) 3974.
[19] V.V. Voronkov, R. Falster, Mat. Sci. Semicond. Proc. 5 (2002) 387.
[20] M. Pagani, R.J. Falster, G.R. Fisher, G.C. Ferrero, M. Olmo, Appl. Phys. Lett. 70 (1997) 1572.
[21] T. M€uller, M. Gehmlich, G. Kissinger, D. Kot, A. Sattler, A. Miller, E. Daub, Phys. Status Solidi C 14 (2017) 1700119.
[22] D. Kot, Brandenbg. Univ. Technol. Cottbus-Senftenberg, Ph.D. Thesis (2013).
[23] R. Falster, D. Gambaro, M. Olmo, M. Cornara, H. Korb, Mater. Res. Soc. Symp. Proc. 510 (1998) 27.
[24] R. Falster, V.V. Voronkov, Mat. Sci. Eng. B 73 (2000) 87.
[25] V.V. Voronkov, R. Falster, J. Cryst. Growth 204 (1999) 462.
[26] V.V. Voronkov, R. Falster, Mat. Sci. Eng. B 134 (2006) 227.
[27] P. Dong, R. Wang, X. Yu, L. Chen, X. Ma, D. Yang, Superlattice Micro. 107 (2017) 91.
[28] J. Coutinho, V.P. Markevich, A.R. Peaker, B. Hamilton, S.B. Lastovskii, L.I. Murin, B.J. Svensson, M.J. Rayson, P.R. Briddon, Phys. Rev. B 86 (2012) 174101.
[29] R.W. Whan, J. Appl. Phys. 37 (1966) 3378.
[30] C.A. Londos, E.N. Sgourou, A. Chroneos, J. Appl. Phys. 112 (2012) 123517.
[31] R. Radu, E. Fretwurst, R. Klanner, G. Lindstroem, I. Pintilie, Nucl. Instrum. Methods Phys. Res. A 730 (2013) 84.
[32] Z. Li, H.W. Kraner, E. Verbitskaya, V. Eremin, A. Ivanov, M. Rattaggi, P.G. Rancoita, F.A. Rubinelli, S.J. Fonash, C. Dale, P. Marshall, IEEE Trans. Nucl. Sci. 39 (1992) 1730.
[33] C.A. Londos, E.N. Sgourou, D. Hall, A. Chroneos, J. Mater. Sci.: Mater. Electron 25 (2014) 2395.
[34] C.A. Londos, A. Andrianakis, E.N. Sgourou, V.V. Emtsev, H. Ohyama, J. Appl. Phys. 109 (2011) 033508.
[35] P. Dong, X. Yu, L. Chen, X. Ma, D. Yang, J. Appl. Phys. 122 (2017) 095704.
[36] Y. Xu, Y. Li, C. Liu, H. Wang, Appl. Phys. Lett. 65 (1994) 2807.
[37] C. Cui, X. Ma, D. Yang, J. Appl. Phys. 104 (2008) 123523.
[38] C. Cui, D. Yang, X. Ma, R. Fan, D. Que, Phys. Stat. Sol. (A) 202 (2005) 2442.
[39] K. Sueoka, J. Electrochem. Soc. 152 (2005) G731.
[40] C.M.- Vinante, E. Ehret, D. Barbier, J. Appl. Phys. 79 (1996) 2707.
[41] D. Kot, G. Kissinger, M.A. Schubert, A. Sattler, Appl. Phys. Lett. 104 (2014) 182101.
[42] A.S. Oates, R.C. Newman, Appl. Phys. Lett. 49 (1986) 262.
[43] S.M. Hu, J. Appl. Phys. 51 (1980) 5945.
[44] A. Borghesi, A. Piaggi, A. Sassella, A. Stella, B. Pivac, Phys. Rev. B 46 (1992) 4123.
[45] O.D. Gryse, P. Clauws, J.V. Landuyt, O. Lebedey, C. Claeys, E. Simoen, J. Vanhellemont, J. Appl. Phys. 91 (2002) 2493.
[46] C. Cui, D. Yang, X. Ma, M. Li, J. Appl. Phys. 103 (2008) 064911.
[47] J. Vanhellemont, C. Claeys, J. Appl. Phys. 62 (1987) 3960.
[48] G. Kissinger, A. Huber, K. Nakai, O. Lysytskij, T. Muller, H. Richter, W. Ammon, Appl. Phys. Lett. 87 (2005) 101904.
[49] W. Ostwald, Z. Phys. Chem. 22 (1897) 289.
[50] A. Sassella, A. Borghesi, P. Geranzani, G. Borionetti, Appl. Phys. Lett. 75 (1999) 1131.
[51] V.V. Voronkov, R. Falster, J. Appl. Phys. 89 (2001) 5965.
[52] H. Wang, X. Ma, J. Xu, X. Yu, D. Yang, Semicond. Sci. Technol. 19 (2004) 715.
[53] X. Ma, L. Lin, D. Tian, L. Fu, D. Yang, J. Phys.: Condens. Mater. 16 (2004) 3563.
[54] S.M. Hu, J. Appl. Phys. 45 (1974) 1567.